Determination of the Electron Density Profile of the Nerve Myelin Membrane in Different States Taking Paracrystalline Lattice Distortions into Account

M. K. Gbordzoe and W. Kreutz

Institut für Biophysik und Strahlenbiologie, Universität Freiburg, Freiburg

Z. Naturforsch. **33 c**, 184–202 (1978) ; received March 7, 1978

Biomembranes, Nerve Myelin, X-Ray Diffraction, Q-Function, Electron Density Profile

Recent investigations point to the presence of paracrystalline lattice disorder in the nerve myelin in the swollen, fixed and to some extent also in the native state. This leads to the distortion of the Q-function of the membrane stack and the Q_0-function of the unit cell, which can be experimentally isolated through swelling.

Representing the distance statistics between neighbouring membranes and the electron density distribution of the single membrane with Gaussian functions, the Q-function can be expressed analytically as a convolution polynomial of the electron density, its mirror image and the distance statistics functions. Fitting this model Q-function to the experimental Q-function obtained by the inverse Fourier transformation of the scattered intensity, one can determine the optimal parameters of the electron density distribution and the distance statistics functions. The elimination of the distance fluctuations between neighbouring membranes permits the calculation of the undistorted Q-function or the Q_0-function. The Fourier Analytical Deconvolution of the undistorted Q_0-function enables a unique determination of the double membrane profile, thus a unique phase determination.

Introduction

Because of its high degree of stacking order and the relative facility with which it can be obtained for investigation, the nerve myelin of peripheral nervous systems has been widely studied by many authors by means of small angle X-ray diffraction methods.

The main difficulty in the interpretation of the diffraction patterns of the nerve myelin has been the assignment of phases to the various diffraction orders.

Different methods have been used by various authors towards the solution of the phase problem: e. g. the swelling and sampling method Finean and Burge [1], Moody [2], Worthington and Blaurock [3], Blaurock [4], Worthington and McIntosh [5], McIntosh and Worthington [6]; the heavy metal labelling technique by Akers and Parsons [7] and Harker [8]. Caspar and Kirschner [9] attempted to determine the correct set of phases by comparing the diffraction patterns of the sciatic and optic nerve myelins of rabbit, assuming the same centrosymmetrical single membrane structure for the various double membrane systems.

With the help of swelling experiments Worthington and McIntosh [5, 10] attempted to determine the profile of the nerve myelin by applying the direct method of Hosemann and Bagchi [11], making use of the intensity functions from different swelling experiments or different swelling states of the nerve myelin to determine the modulus of the continuous Fourier transform of the electron density of the membrane pair (unit cell).

In order to calculate the autocorrelation function of the unit cell, the so-called Q_0-function, McIntosh and Worthington [6, 10] found it essential to introduce a 'fictitious repeat period' which was large enough to permit the Q_0-function to decay to zero at about 160 Å. Further, the deconvolution procedure employed by these authors – the so-called 'relaxation' method [5] does not permit a unique phase determination [10]. These factors limit the application of the method considerably.

In most earlier investigations, it has usually been assumed that the nerve myelin membrane system does not undergo any lattice distortions upon swelling.

Our investigations and those of others [12, 13] recently have shown that the nerve myelin membrane system in the swollen, fixed and to some extent even in the natural state shows considerable paracrystalline lattice distortions [11] as evident from careful analysis of the electron micrographs and line broadening in the scattered intensities of nerve myelin samples. Thus, the neglection of lattice distortions (distance statistics between neighbouring membranes) hitherto is not generally justifiable.

Requests for reprints should be sent to Prof. Dr. W. Kreutz, Institut für Biophysik und Strahlenbiologie der Universität, Albertstr. 23, D-7800 Freiburg.

In the present investigation, the electron density profiles of the nerve myelin membrane in various states (swollen, fixed and native) have been determined directly with the help of the so-called Q-function method of Hosemann and Bagchi [11], taking into account the influence of paracrystalline lattice distortions within the membrane system.

Due consideration has been given not only to distance statistics between adjacent double membranes, but also to centre-to-centre distance fluctuation within the unit cell itself.

The method consists essentially of the following three steps: Firstly, the experimental determination of the Q-function of the membrane stack through the inverse Fourier transformation of the experimental intensity function after appropriate corrections.

The experimental Q-functions are perturbed, *i. e.* the Q-function no longer has an exact periodicity and the peaks are smeared with increasing period because of distance statistics within the membrane system.

Secondly, with the help of model electron density profiles ('trial functions') the optimal parameters of the electron density distribution of the single membrane and the distance statistics are calculated in a Patterson synthesis employing an iterative Non-Linear Least-Square-Refinement Procedure according to Marquardt [14]. With these calculated distance statistics, the lattice distortions or distance fluctuations can be eliminated from the experimental Q-functions. One can obtain the undistorted Q-functions (or Q_0-functions).

Thirdly, applying the Fourier Analytical Deconvolution Method (FAD-Method, Pape [15]), the electron density distribution of the membrane pair can be determined by deconvoluting the undistorted Q_0-function.

This procedure for determining the electron density, termed the Phasing-In-Procedure or SM-FAD-"Statistically Modified Fourier Analytical Deconvolution"-Method [16] permits:

1) the determination of the electron density distribution of the myelin stack including the interspaces and the corresponding distance statistics in various experimental states (swollen, fixed and native);
2) a unique determination of the phases of the structure amplitude, *i. e.* a unique determination of the electron density profile of the double membrane in different states;
3) a qualitative and quantitative description of the effects of various swelling solutions or fixatives on the double or single membrane profiles of the live nerve.

Description of the Myelin System with the Q-Function Formalism

General description

From the point of view of X-ray crystallography, the nerve myelin membrane system can be represented approximately as a one-dimensional lattice structure with identical centrosymmetrical lattice cells.

The inverse Fourier transformation of the scattered intensity of the myelin stack in the natural state – corresponding to a paracrystal with a large number of unit cells – gives rise to a 'quasi-periodical' Patterson-function (the Q-function), which decreases only very slowly with increasing distance.

As demonstrated firstly by Hosemann and Bagchi [11], for a crystal with a small number of centrosymmetrical cells, the Q-function takes a form termed by Hosemann as the "tile structure" (Fig. 1).

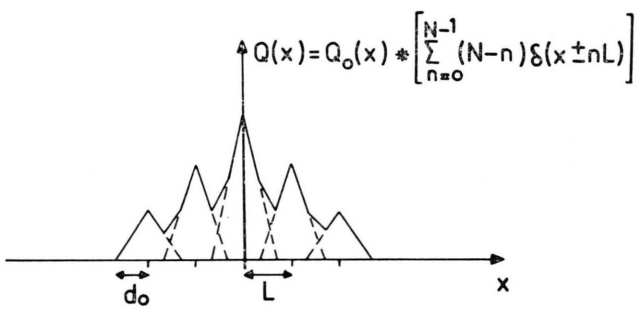

Fig. 1. 'Tile structure'. The Q-function of a crystal with a small number of unit cells. It consists of a series of Q_0-functions with decreasing amplitudes at successive lattice points nL.

In the absence of paracrystalline lattice distortions, it can be shown that the Q-function is given by the relation:

$$Q(x) = \varrho(x) * \varrho(-x)$$
$$= Q_0(x) * \sum_{n=0}^{N-1} (N-n)\,\delta(x \pm n\,L) \qquad (1)$$

where

$\varrho(x)$ is the electron density distribution of the membrane stack, N the number of unit cells in the

crystal and L the lattice constant. δ denotes the Dirac's Delta function.

$$Q_0(x) = \varrho_0(x) * \varrho_0(-x) = \overset{2}{\sim}\varrho_0 \tag{2}$$

is the convolution square of the electron density of the unit cell (double membrane); $*$ denotes convolution, $\overset{2}{\sim}$ the convolution square; ϱ_0 is the electron density distribution of the double membrane.

If d_0 denotes the extension of ϱ_0 in the x-direction, then the extension of Q_0 is $2\,d_0$ (see Fig. 1).

According to Eqn (1) the Q-function is composed of a series of Q_0-functions which are convoluted $n+1$ fold about successive lattice points $(N-n)$.

Separation of the Q_0-function

The above considerations give a possibility for the separation of the Q_0-function, using either mathematical artifices – Kreutz [17 a, b], Lesslauer, Cain and Blasie [18] or experimental methods such as swelling – among others, Blaurock [4], Worthington and McIntosh [10]. In these earlier attempts to obtain the autocorrelation function of the unit cell, the influence of distance statistics between neighbouring membranes had generally been neglected.

The Q-function of the nerve myelin membrane system in the presence of distance statistics

Fig. 2 shows a schematic representation of the nerve myelin system in the natural and swollen state and the correlation of the distance statistics

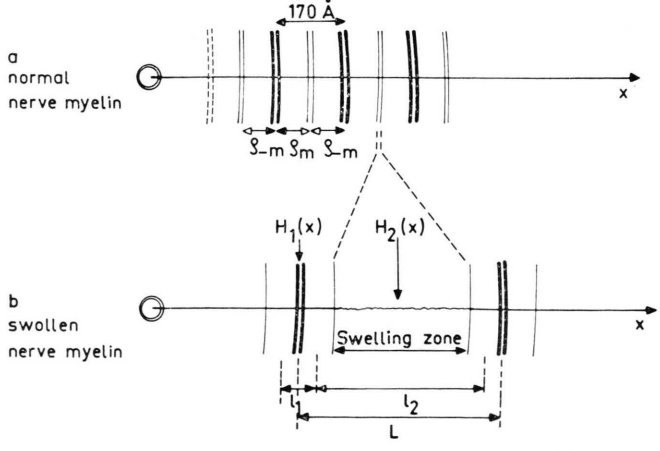

Fig. 2. Diagrammatic representation of unswollen and swollen nerve myelin systems with the correlation of the distance statistics functions $H_1(x)$ and $H_2(x)$ to the cytoplasmic and extracellular interspaces.

functions $H_1(x)$ and $H_2(x)$ respective to the cytoplasmic and extracellular interspaces. From electron microscopic observations it has been concluded that the swelling in glycerol and sucrose occurs in the extracellular interspace.

The x-coordinate denotes the radial direction, ϱ_m is the projection of the electron density distribution of a single membrane on the stacking axis and ϱ_{-m} its mirror image. When only the relative electron density distribution of the membrane stack is being considered, the electron density of the swelling zone (of constant fluid electron density) can be set equal to zero.

We make use of the following definitions: Convolution product of $f_1(x)$ with $f_2(x)$ (see for example H. Margenau, G. M. Murphy [19]

$$f_1(x) * f_2(x) = \int_{-\infty}^{\infty} f_1(t) f_2(x-t)\,\mathrm{d}t; \tag{3}$$

convolution square of a function:

$$f(x) * f(-x) = \int_{-\infty}^{\infty} f(t) f(t-x)\,\mathrm{d}t.$$

Without distance statistics, the electron density distribution of a membrane pair in the unswollen state can be represented by the following relations:

$$\varrho_0(x) = \varrho_{-m} + \varrho_m * \delta(x - l_i) \tag{5}$$

e. g. for a face-to-face coupling and

$$\varrho_0'(x) = \varrho_m + \varrho_{-m} * \delta(x - l_j) \tag{6}$$

for a back-to-back coupling,
where l_i and l_j are respectively the centre-to-centre distance in the two cases. δ denotes the Dirac's Delta function.

Since the $Q(x)$ is always centrosymmetrical, we restrict the presentation in the following to only the positive x-direction.

From Eqns (2), (5), and (6) one obtains for the Q_0-function the following relations:

$$\begin{aligned} Q_0(x) &= \varrho_0(x) * \varrho_0(-x) \\ &= 2\overset{2}{\sim}\varrho_m + \varrho_m * \varrho_m * \delta(x - l_i) \\ &\qquad x > 0 \end{aligned} \tag{7}$$

for a face-to-face coupling of the single membranes or

$$\begin{aligned} Q_0' &= 2\overset{2}{\sim}\varrho_m + \varrho_{-m} * \varrho_{-m} * \delta(x - l_j) \\ &\qquad x > 0 \end{aligned} \tag{8}$$

for the back-to-back coupling of the single membranes.

In the case of lattice distortions, the Delta functions in Eqn (5), (6), (7), and (8) are replaced by the distance statistics functions $H_1(x)$, $H_2(x)$ [20].

In this case one obtains the relations:

$$Q_0(x) = 2\overset{2}{\widetilde{\varrho_m}} + \varrho_m * \varrho_m * H_1(x) \tag{9}$$

for a face-to-face coupling or

$$Q_0'(x) = 2\overset{2}{\widetilde{\varrho_m}} + \varrho_{-m} * \varrho_{-m} * H_2(x) \tag{10}$$

for a back-to-back coupling.

For a swollen nerve myelin system if $H_1(x)$ denotes the distance statistics within the membrane pair * then $H_2(x)$ denotes the distance statistics between the membranes coupled by the swelling zone.

As distance statistics functions we introduce the Gaussian distribution functions

$$H_1(x) = A_1 e^{-c_1(x-l_1)^2} \tag{11}$$

$$H_2(x) = A_2 e^{-c_2(x-l_2)^2} \tag{12}$$

where l_1 and l_2 are the average centre-to-centre distances between neighbouring membranes (see Fig. 2).

The sum of l_1 and l_2 is equal to L, the average Bragg distance (lattice constant).

By considering only one neighbouring unit cell, $H_1(x)$ and $H_2(x)$ are normalized according to the relations [21].

$$\int_{-\infty}^{\infty} H_i(x)\,dx = 1\,. \tag{13}$$

From Eqns (11), (12), and (13) one then obtains

$$A_1 = \left[\frac{c_1}{\pi}\right]^{\frac{1}{2}} \qquad A_2 = \left[\frac{c_2}{\pi}\right]^{\frac{1}{2}}. \tag{14}$$

By considering Eqn (1) in the presence of lattice distortions of the second kind, the $Q(x)$-function can be expressed as a convolution polynomial of the electron density distribution of the single membrane $\varrho_m(x)$, its mirror image $\varrho_{-m}(x)$ and the distance statistics functions $H_1(x)$ and $H_2(x)$.

For convenience, we introduce the following abbreviations:

$$Q_m(x) \equiv Q_m = \varrho_m * \varrho_{-m} = \overset{2}{\widetilde{\varrho_m}} \tag{15}$$

$$Q_{m1}(x) \equiv Q_{m1} = \varrho_m * \varrho_m \tag{16}$$

$$Q_{m2}(x) \equiv Q_{m2} = \varrho_{-m} * \varrho_{-m}\,. \tag{17}$$

* It must be emphasized that distance fluctuation within the unit cells composing the swollen myelin, owing to the swelling mechanism, causes the distortion of the Q_0-function of the unit cell compared with the natural state.

For the entire model $Q(x)$-function – corresponding to N cytoplasmatic interspaces, $N-1$ extracellular interspaces and $2N$ single membranes – one obtains in place of Eqn (1) the new relation:

$$\begin{aligned} Q(x) = {} & 2N Q_m * \delta(x-0) + N Q_{m1} * H_1 \\ & + (N-1) Q_{m2} * H_2 \\ & + (N-1)\,2\,Q_m * H_1 * H_2 \\ & + (N-1) Q_{m1} * H_1 * H_2 * H_1 \\ & + \sum_{n=2}^{N-1} (N-n)\{Q_{m1} * H_1 * H_2 * H_1 \\ & + Q_{m2} * H_2 \\ & + 2\,Q_m H_1 * H_2\} * (H_1 * H_2)_{n-1} \end{aligned} \tag{18}$$

where $(H_1 * H_2)_n$ means the n-fold convolution product of $(H_1 * H_2)$.

In the case of nerve myelin, it has been found sufficient to use only the first four terms in Eqn (18) – describing the Q-function from $x=0$ to $x=L$ – for the calculation of the electron density distribution of the membrane system in the swollen, fixed and normal states.

In this case, N can be eliminated from the equation by putting $N-1 \cong N$ and dividing both sides of the equation with N. The corresponding Q-function is then given by the relation:

$$\begin{aligned} Q(x)_L = {} & 2\,Q_m * \delta(x-0) + Q_{m1} * H_1 \\ & + Q_{m2} * H_2 + 2\,Q_m * H_1 * H_2\,. \end{aligned} \tag{19}$$

The Phasing-in-Procedure

The non-linear least-square procedure

The model electron density of a single membrane $\varrho_m(x)$ is represented as a sum of Gaussians $G(A_i, x_i, c)$ with the same width c according to the relation:

$$\varrho_m(x) = \sum_i A_i e^{-c(x-x_i)^2}. \tag{20}$$

The number of Gaussians to be used was chosen with the help of the formular given by Buerger [22] relating the number of peaks in the Patterson function – here the Q-function – to the number of peaks in the electron density distribution.

It was found sufficient to use a sum of 3 Gaussians to describe the electron density distribution of the single membrane.

Starting with an initial set of parameters (A_i, x_i, c) for ϱ_m and (c_i, l_i) for $H_i(x)$ the optimal values for ϱ_m and (c_i, l_i) were found by a Non-Linear Least-Square refinement procedure [14], which

minimizes the sum of the squares of the differences between the experimental $Q(x)$-function, $Q(x_i)_{exp}$ and the model $Q(x)$-function $Q(x_i)_{mod}$ according to the equation:

$$\Phi = \sum_{i}^{N^*} (Q(x_i)_{exp} - Q(x_i)_{mod})^2 . \quad (21)$$

$Q(x)_{exp}$ is determined by the inverse Fourier transformation of the scattered intensity while $Q(x)_{mod}$ is calculated according to Eqn (19). N^* is the number of values of $Q(x)_{exp}$ used for the Least Square procedure.

For comparing the degree of agreement between Q_{exp} and Q_{mod} for various experimental conditions of the nerve myelin, we introduce the parameter G defined by the relation:

$$G = \frac{Q_{N^*}}{N^*} = \frac{1}{N^*} \sum_{i}^{N^*} (Q_{exp} - Q_{mod})^2 . \quad (22)$$

The half widths c_i of the distance statistics functions $H_i(x)$, give a measure of the degree of distortion within the various systems.

The relative average fluctuation of the centre-to-centre distances between neighbouring membranes is given by the relation:

$$g_i = \frac{\Delta_i}{\bar{l}_i} = \frac{1}{\bar{l}_i [2\, c_i]^{1/2}} , \; i = 1, 2 . \quad (23)$$

Elimination of the perturbation of the Q-function

Using the centre-to-centre distances l_1 and l_2 one can eliminate the distance fluctuation in the experimental $Q(x)$ – functions by replacing the $H_1(x)$ and $H_2(x)$ functions with Delta-functions $\delta(x - l_1)$ and $\delta(x - l_2)$ respectively.

This enables the calculation of the undistorted Q_0-functions for the double membranes in any state, using Eqns (9) or (10).

Deconvolution and phasing

By deconvoluting the undistorted Q_0-functions with the Fourier Analytical Deconvolution Method [15] one can obtain a unique solution for the electron density distribution of the double membrane in any experimental state. Both the Bragg distance and the centre-to-centre distance between neighbouring membranes can be assumed to be strictly constant.

The electron density distribution of the membrane stack is ideal periodical and the double membrane profile shows no deviation from centro-symmetry. Since this situation is the ideal case, we denote the electron density distribution of the double membrane as "ideal'.

The Fourier coefficients $C(\bar{h}, \bar{k}, \bar{l})$ in the Fourier series representation of the electron density distribution in the FAD-Method can directly be related to the structure amplitudes $F(h, k, l)$ of the scattered intensity both in modulus and sign [23, 24] using the equation:

$$F(h\,k\,l) = C(\bar{h}\,\bar{k}\,\bar{l})\,V$$

where V is the volume of the unit cell of space lattice. It follows, that the FAD deconvolution method is equivalent to phasing, the phases of the structure amplitude being unique for undistorted Q_0-functions.

Methods

Samples

As samples, we used sciatic nerves of frog (*Rana esculenta*) in the natural, swollen and fixed states. For the natural state (live nerve), nerve myelin samples in isotonic Ringer's solution were used, while for the swelling experiments nerve samples were swollen after dissection for about 24 to 48 h in solutions of 6.5% glycerol (compare with Worthington and McIntosh [10]) or 0.8 M sucrose at 4 °C. For the fixation experiments nerve myelin samples fixed in Osmiumtetroxide vapour about 1 min were investigated.

For irradiation, the myelin samples were placed in Mark capillary tubes 1.0 mm in diameter and 10 μm wall thickness filled with either Ringer's solution or with the swelling solution.

In order to test the effect of the swelling process on the electron density profile of the membrane stack, swollen nerve samples were reimmersed in isotonic Ringer's solution for about 24 h in order to reverse the swelling before irradiation. Such samples are termed pseudonatural (or pseudo live nerve).

All samples were irradiated at room temperature.

X-ray equipment and recording

As X-ray sources, a Philips fine structure generator Mueller Mikro III, and Rigaku X-ray diffraction generator Rota Unit RU-200 PL (rotating anode) were employed. The small angle X-ray diffraction patterns were recorded with Kiessig [25] and

Kratky [26] small angle cameras in conjunction with AGFA Structurix DC and Alford Industrial G films, using Cu-Kα-line filtered with Ni-filter or a Quarz monochromator.

All samples were irradiated with point-collimated primary beams. A main disadvantage in using a point-collimated X-ray beam was the very long exposure time required for the recording. However, control experiments had shown that the nerve myelin sheath is structurally very stable: even after a week, the Bragg reflections did not change appreciably.

The sample to film distance in the various experiments ranged from 20 to 23 cm. The intensity profiles were recorded with a Joyce Loebl double beam Micro densitometer, model MK III c.

Diffraction patterns

Low angle-X-ray diffraction patterns of normal, swollen and fixed nerve myelin samples are shown in Figs 3 to 6.

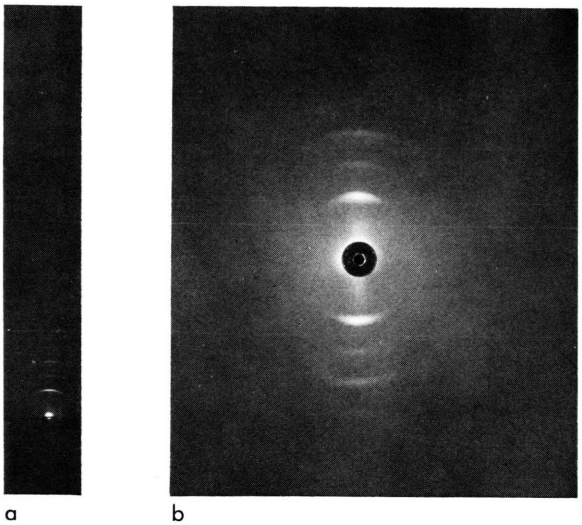

Fig. 3. Meridian reflections of normal nerve myelin, in isotonic Ringer's solution. a) Kratky camera recording, exposure time $t_e=72$ h; b) Kiessig camera recording, exposure time $t_e=3$ h.

Fig. 4. Diffraction pattern of myelin sample swollen in 0.8 m sucrose solution; swelling time $t_{sw}=53$ h, exposure time $t_e=75$ h.

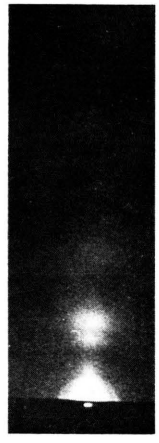

Fig. 5. Diffraction pattern of myelin sample swollen in 6.5% glycerol; swelling time = 27½ h, exposure time = 225 h.

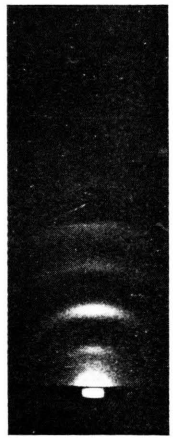

Fig. 6. Diffraction pattern of a nerve myeling sample fixed for 1 min in OsO_4 vapour; exposure time=159 h.

Densitometer Tracing

With live nerve in isotronic Ringer's solution, the well known 5 principal sharp reflections on a smooth and monotonically decreasing back-ground scattering, B, are obtained (Fig. 7). With pseudo live nerve, the principal reflections in isotonic Ringer's solution are somewhat broader (Fig. 8) than in the case of native myelin. This indicates greater disorder in the membrane system due to some residual effect of the swelling. The Bragg period in the two cases in approximately 171 Å.

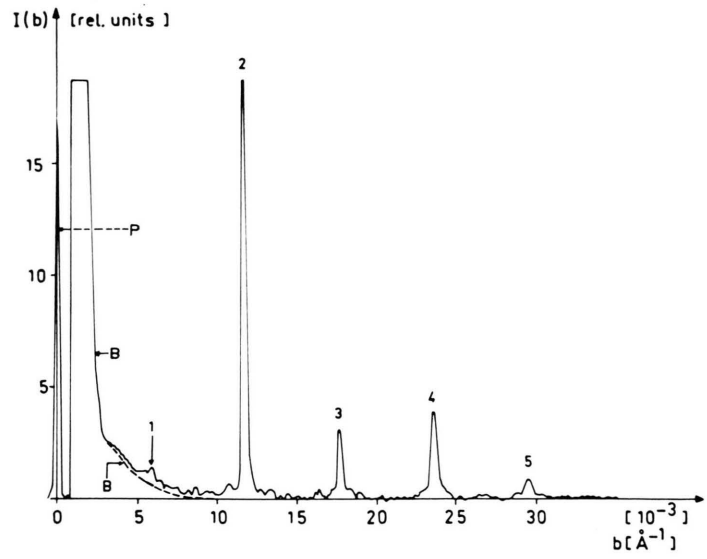

Fig. 7. Intensity function and the background scattering curve, B, of live nerve corresponding to the diffraction pattern in Fig. 3 a P ≡ primary beam.

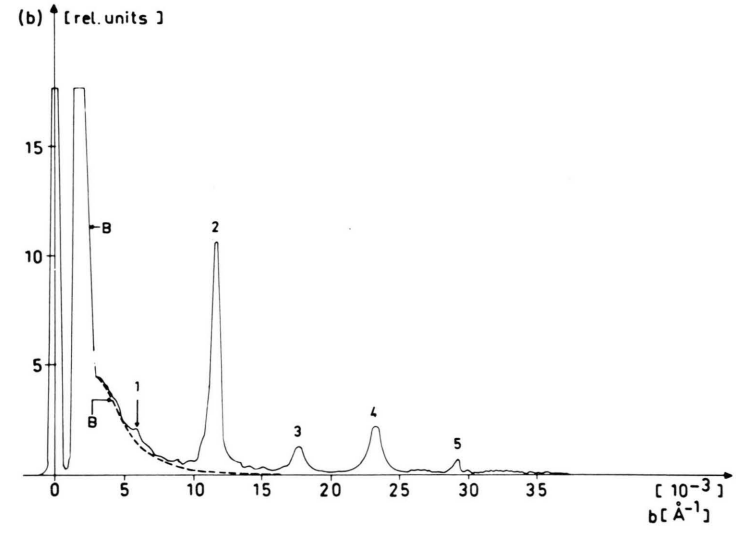

Fig. 8. Intensity function of pseudo-normal nerve, swollen in 6.5% glycerol for 28 h and reimmersed in isotonic Ringer's solution for $3^1/_2$ days before irradiation. B represents the background scatterng curve.

The background scattering can be attributed to several factors:

a. capillary tube with solution in which the specimen is positioned for irradiation;
b. the non-lamellar parts of nerve.

The scattering due to the capillary tube and the solution can be corrected for experimentally by recording the scattered intensity without the sample ('Blind recording'). This has generally been found to be negligible.

On account of the partial orientation of the myelin system giving rise to arcs of circles as diffraction patterns in the case of a point collimated primary beam (Figs 3 – 6), the back-ground scattering due to the non-lamellar portions of the sample can be obtained approximately by taking densitometer tracings in a radial direction along the edges of the arcs in such a way that the peaks of the highest intensity profiles just disappear. These background scattering curves are indicated on the scattered intensity functions with broken lines B. The difference between the background scattering and the densitometer tracing along the meridian gives the scattered intensity of the lamellar system.

On swelling, the Bragg repeat period increases from about 171 Å in the natural state to about 361 Å after 53 h swelling in 0.8 M sucrose solution (Fig. 9) and about 298 Å after about 28 h swelling

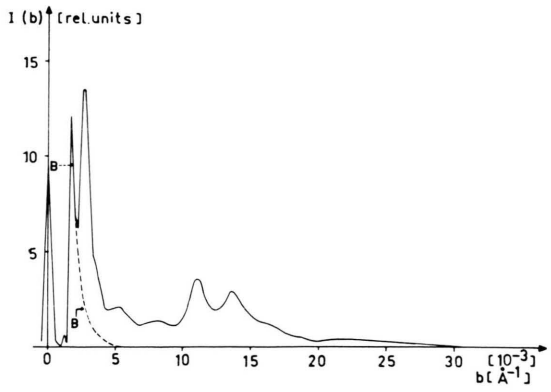

Fig. 9. Intensity function of myelin swollen in 0.8 m sucrose corresponding to diffraction pattern in Fig. 4. B denotes the background scattering curve.

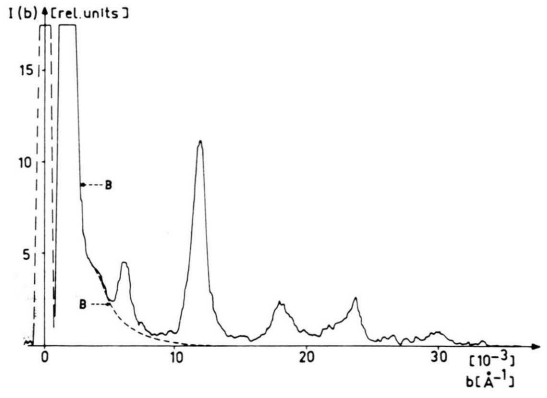

Fig. 11. Intensity function and the background scattering curve B, of myelin fixed for 1 min in OsO_4-vapour.

in 6.5% glycerol solution (Fig. 10). The Bragg period of the myelin system decreases to about 166 Å on 1 min fixation in osmiumtetroxide vapour (Fig. 11).

The values of the Bragg periods d_n, calculated for the different diffraction orders n of the same intensity curve, vary with n (Table I). Further there is appreciable increase in the half width of the reflection profiles with increasing order of diffraction.

Both effects are due to paracrystalline lattice distortions [11].

Regarding swollen nerves, it was observed that the higher orders are no longer well resolved (Figs 9 and 10). With increasing distance statistics of the order of 25 to 35% [27, 28], diffraction orders higher than the first appear smeared and become indistinguishable from the background.

Table I. Variation of Bragg distance with diffraction order.

n d_n [Å] [a]	d_n [Å] [b]	d_n [Å] [c]
1 169	364	162
2 172	368	167
3 171	368	165
4 171	356	168
5 170	362	166
$\bar{d}$=170 Å	$\bar{d}$=362 Å	$\bar{d}$=166 Å

[a] Fresh live nerve; [b] nerve sample swollen in 0.8 M sucrose solution; [c] live nerve fixed for 1′ in OsO_4-vapour.

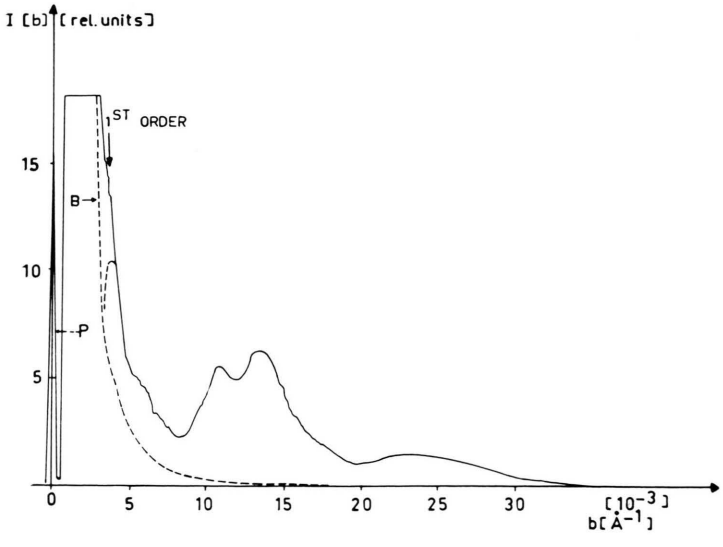

Fig. 10. Intensity function and the background scattering curve of myelin sample swollen in 6.5% glycerol, corresponding to the diffraction pattern in Fig. 5. P ≡ primary beam.

By using the smallest possible slit at our disposal (20 μ) for collimating the X-ray primary beam, it has been observed that even with live nerve, there is a slight increase in the half-width of the intensity profiles with increasing diffraction order.

Thus, in our calculations we take into account distance statistics not only in the case of swollen and fixed nerves but also in live nerve myelin systems. We denote the distance statistics present in the normal membrane system as intrinsic or 'Eigen' statistics. Comparison of the scattered intensity curves indicate that swelling and fixation cause additional distortions in the lamellar system.

Results

Direct determination of the Q_0-function of swollen nerve myelin

The experimental $Q(x)$ function is obtained by the inverse Fourier transformation of the scattered intensity according to the equation:

$$Q(x)_{\text{exp}} = 2 \int_0^{b_{\max}} (I(b)_{\text{corr}}) \cdot \cos\,(2\,\pi\,b\,x)\,\mathrm{d}b \quad (24)$$

where $I(b)_{\text{corr}}$ represents the corrected intensity function, b the scattering vector in reciprocal space with modulus b equal to $2\,\Theta/\lambda$ for small scattering angles $2\,\Theta$.

For small angle scattering experiments using a small point-collimated primary beam, both collimation and polarization corrections can be neglected. The Lorentz-factor for a system employing a monochromatic point-collimated X-ray primary beam for irradiating the myelin sheath can be shown to be $1/b^2$ (compare Fig. 3 b with a Debye Scherrer System), for example Hosemann and Bagchi [11], Neff [29], Azároff [24].

Thus,

$$I(b)_{\text{corr}} = I(b)_{\text{exp}}\, b^2 \quad (25)$$

where $I(b)_{\text{exp}}$ is the experimentally determined scattered intensity.

Fig. 12 shows an example of the corrected intensity function of a swollen nerve obtained by multiplying the experimental scattered intensity in Fig. 9 with b^2 (point collimation) according to Eqn (25).

Fig. 13 shows the corresponding Q-function with the Q_0-function obtained through the inverse Fourier transformation of the corrected intensity function in Fig. 12.

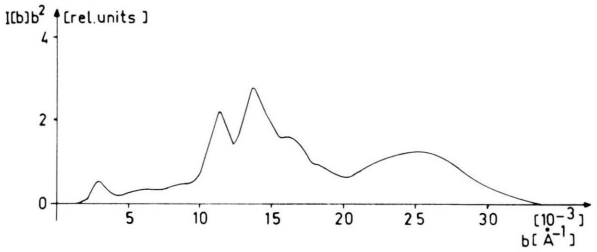

Fig. 12. Corrected intensity function of myelin swollen in 0.8 M sucrose.

The direct deconvolution of Q_0-function in Fig. 13 with the FAD-method, without considering the effect of distance statistics, gives a double membrane profile as shown in Fig. 14 a. This represents the electron density distribution, when the distortion of the Q_0-function, resulting from distance fluctuation within the membrane pairs in the swollen nerve, is about 10% (see Table V a). In this case, all the Fourier coefficients corresponding to the phases of the major reflections are *plus*. – Compare with Fig. 25, 1, Z_1.

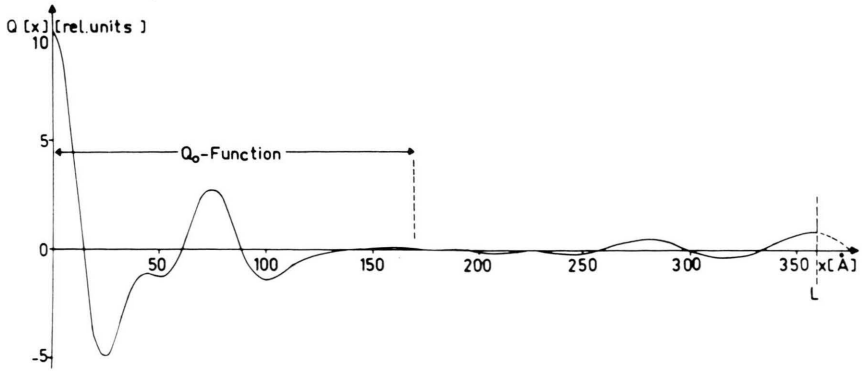

Fg. 13. The Q-function of myelin swollen in 0.8 M sucrose showing the experimentally isolated Q_0-function for $L \geqq 2\times$ double membrane width.

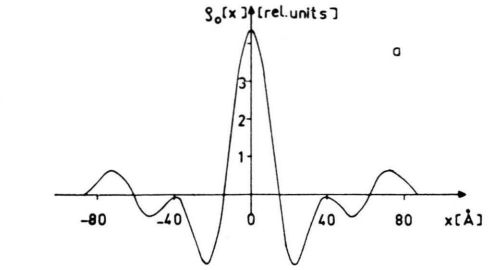

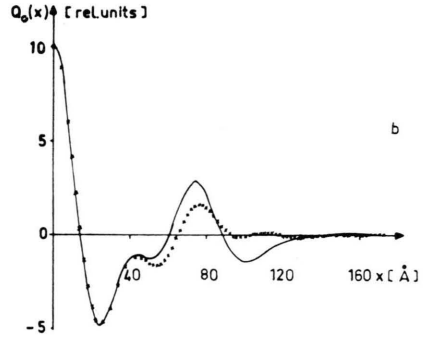

Fig. 14 a. Double membrane profile of myelin swollen in 0.8 M sucrose, obtained by deconvoluting the Q_0-function without taking lattice disorder into account.

Fg. 14 b. —— = experimental Q_0-function, $\times\times\times$ = the model Q_0-function corresponding to the double membrane profile computed with the FAD-Method.

The corresponding model Q_0-function is compared with the experimental Q_0-function in Fig. 14 b. The discrepancy between the two Q_0-functions should be noted.

Determination of ϱ_m, c_i and l_i with the least square refinement procedure

Examples of the optimal parameters of ϱ_m and the Φ and G-values obtained according to the Least-Square-Refinement-Procedure for swollen, live and fixed nerves are given in Tables II a, b, c, d, and e.

The corresponding electron density profiles $\varrho(x)$ with the interspaces, the distance statistics functions and the Q-functions are shown in Figs 15 to 19. The experimental Q-functions are represented by continuous curves (−) while the model Q-functions are indicated with crosses (×). The model electron density profiles of the membrane stack in the swollen state consist of a sequence of double membranes separated by a large swelling zone of constant fluid density (Figs 15, 16).

For the unswollen nerve myelin membrane system (Fig. 17), one obtains a series of images and mirror images in a closed face-to-face and back-to-back contacts. Various membrane parameters for swollen, fixed and normal nerves are compared in Table III.

Table II. Examples of the optimal values of ϱ_m, Φ and G-values. Φ and G are referred to $Q_{exp}(max) = 10$.

a) Nerve myelin swollen in 0.8 M sucrose ($L = 361$ Å)

i	A_i	x_i	c	Φ	$G(10^{-2})$
1	1.9011	−22.2836	0.0092	4.38	2.433
2	−2.0608	0.0	0.0092		
3	0.8634	22.7680	0.0092		

b) Nerve myelin swollen in 6.5% glycerol solution ($L = 298.7$ Å)

i	A_i	x_i	c	Φ	$G(10^{-2})$
1	1.9406	−23.0247	0.0137	3.34	2.256
2	−2.2413	0.0	0.0137		
3	0.9681	21.8091	0.0137		

c) Frog live nerve ($L = 170.4$ Å)

i	A_i	x_i	c	Φ	$G(10^{-2})$
1	1.0888	−24.5734	0.0072	0.65	0.7558
2	−2.6303	0.0	0.0072		
3	1.6169	16.1174	0.0072		

d) Pseudo normal nerve (swelling in 6.5% glycerol solution and reversal of the swelling in isotonic Ringer's solution $L = 171$ Å)

i	A_i	x_i	c	Φ	$G(10^{-2})$
1	1.0451	−23.0972	0.0125	0.83	0.9651
2	−2.3909	0.0	0.0125		
3	1.6540	21.3595	0.0125		

e) Nerve myelin fixed in OSo_4 vapour for 1 min ($L = 168$ Å)

i	A_i	x_i	c	Φ	$G(10^{-2})$
1	1.1193	−18.6026	0.0151	4.6	5.505
2	−2.3802	0.0	0.0151		
3	1.7957	22.7741	0.0151		

Determination of the double membrane profiles through the deconvolution of the unperturbed Q_0-function with the SM-FAD-method

Swollen nerve:

The ideal electron density distribution of the double membrane obtained by deconvoluting the unperturbed Q_0-functions (after elimination of the distance statistics) for swollen nerves are shown in Figs 20 and 21.

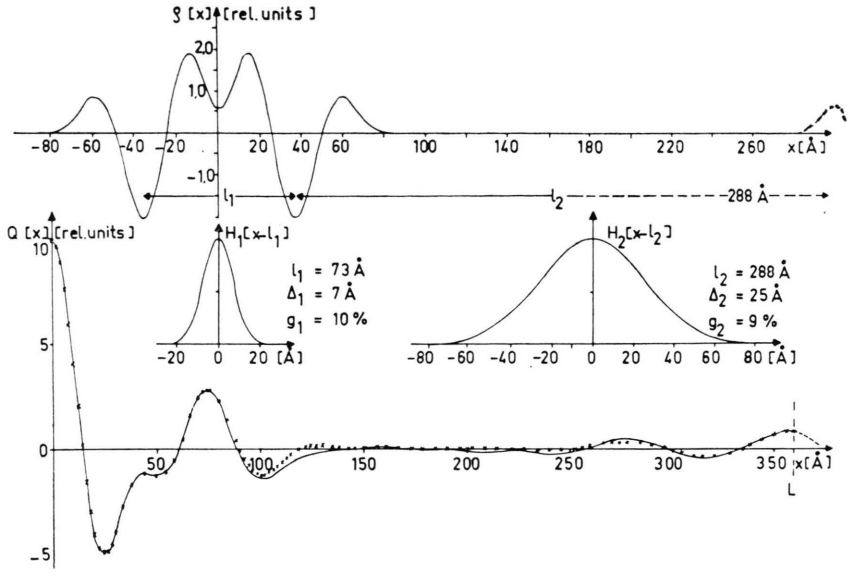

Fig. 15. The electron density distribution of myelin swollen in 0.8 M sucrose with the interspaces, the corresponding distance statistics and the Q-functions. Compare with Fig. 14.

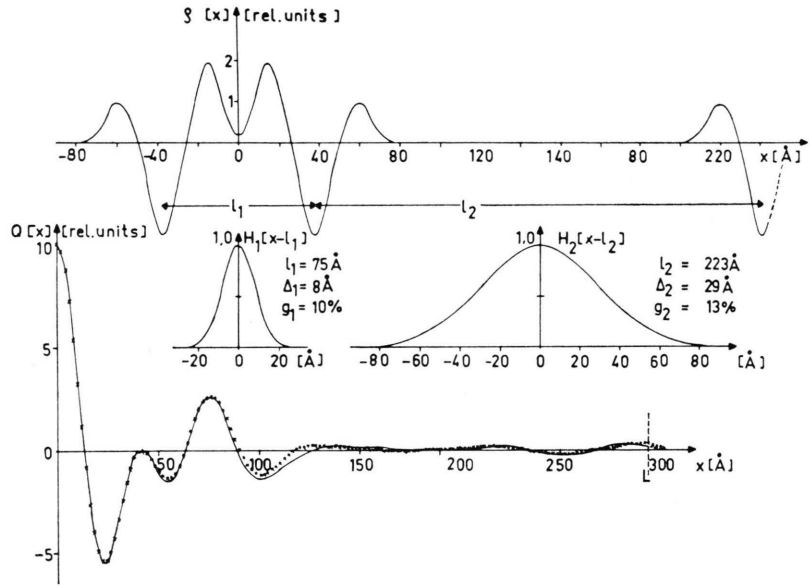

Fig. 16. The electron density distribution of myelin system swollen in 6.5% glycerol with the interspaces, the corresponding distance statistics and the Q-functions.

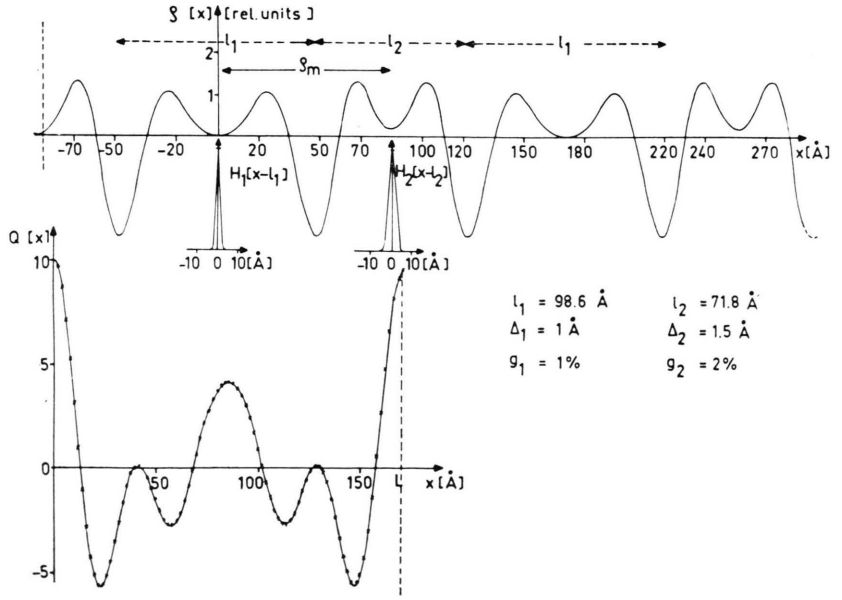

Fig. 17. The electron density distribution, the distance statistics and the Q-functions of live myelin system. Note the relatively narrow distance statistics functions compared with swollen myelin systems. In live nerve, the extracellular interspace shows a smaller distance statistics function than the cytoplasmic interspace.

Table III. Some membrane parameters for swollen, live and fixed nerve samples.

Nerve sample	l_{cp}	DMW_1	DMW_2	l_{00}	l_{i0}	L_0	d [Å]
swollen in 0.8 M sucrose	74	162	164	118	45	361.3	362
swollen in 6.5% glycerol	74.8	148–160 *	156–158	120	45	298	(d_4=298.5)
live nerve	71.8	168–170	168–170	121	43	170.4	170.5
pseudo-live nerve	75.8	158–160	162	122	45	171	171
1′-fixation in OsO_4-vapour	74.7	140	144–146	112	41	168	166

All distances are in (Å)

l_{cp} = Average centre-to-centre distance across the cytoplasmic interspace.

$DMW_{1,2}$ = Double membrane width $\begin{cases} 1 \equiv \text{from the Least-Square Procedure; } Q\text{-function distorted.} \\ 2 \equiv \text{from the undistorted } Q_0\text{-function } **. \end{cases}$

l_{00} = Distance between the positive outside peaks of the double membrane.

l_{i0} = Distance between the positive peaks (inside-outside) of the single membrane.

L_0 = Repeat distance of the double membrane system calculated with the Least-Square-Refinement Procedure.

d = Average repeat distance calculated with the Bragg equation.

* Uncertainty in the exact location of the 1st diffraction order in the case of myelin swollen in glycerol because of the 'overlapping' continuous scattering results in some error in the determination of the DMW. 148 Å was the minimum obtained from several experiments, the entire intensity function — from the 1st to higher diffraction orders — having been used for calculating the Q-function. If only the 3rd and higher orders were used in comparison with McIntosh and Worthington [5] — Fig. 2, page 98 — one obtaines about 160 Å, which agrees with the value reported by these authors [6].

** These values are more accurate since the Q_0-function is undistorted.

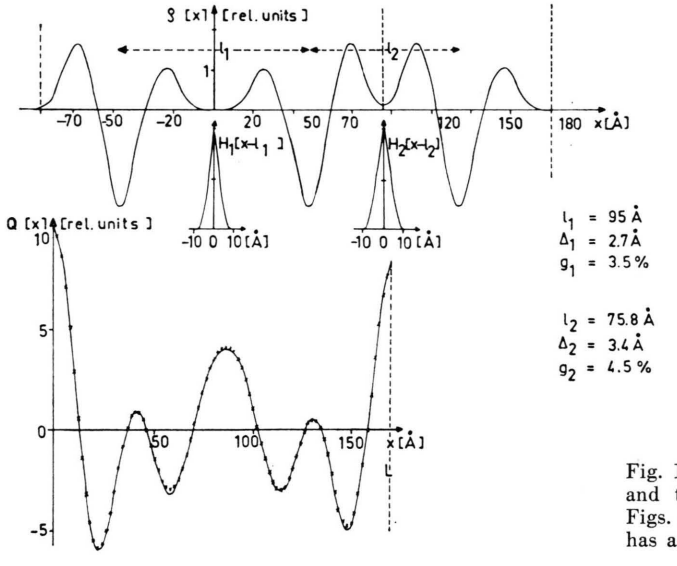

Fig. 18. Electron density distribution, the distance statistics and the Q-functions of pseudo-live nerve. Comparison of Figs. 17 and 18 indicates that pseudo normal myelin system has a larger degree of disorder than live myelin.

The undistorted Q_0-functions calculated from the experimental Q-functions according to Eqn (9) are shown by the continuous curves (–). The model Q_0-functions computed with the FAD-method are indicated by crosses (×).

Natural nerve:

By extending the SM-FAD-method to the normal myelin system, the Q_0-functions of the double membrane for both back-to-back and face-to-face pairing have been calculated from the Q-function of live nerve according to Eqns (9) and (10) respectively, where the distance statistics functions $H_i(x-l_i)$ tend to $\delta(x-l_i)$. The results are shown in Fig. 22 a, b.

Since the two curves are not identical, it is easy to determine the required Q_0-function of the double membrane either through comparison with the Q-function of live nerve — from $x=0$ to $X=L$, or

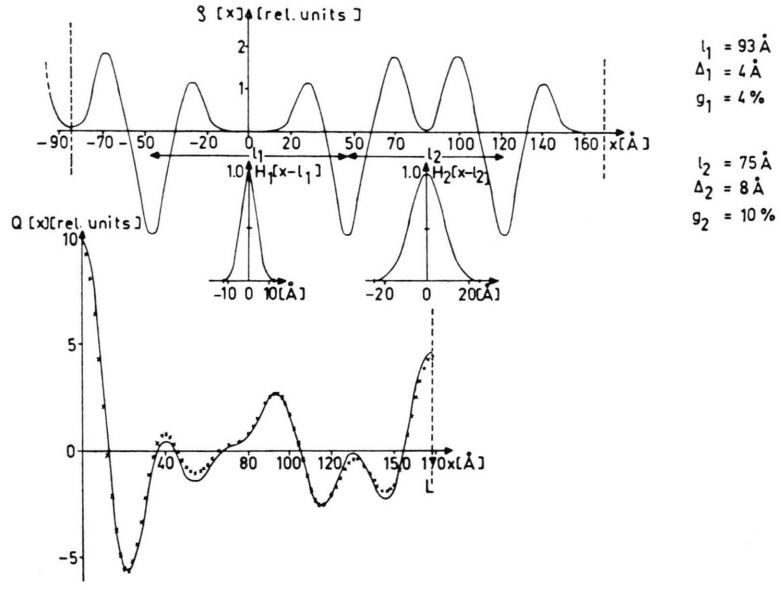

Fig. 19. Electron density distribution, distance statistics and Q-functions of myelin fixed for 1 min in OsO_4-vapour.

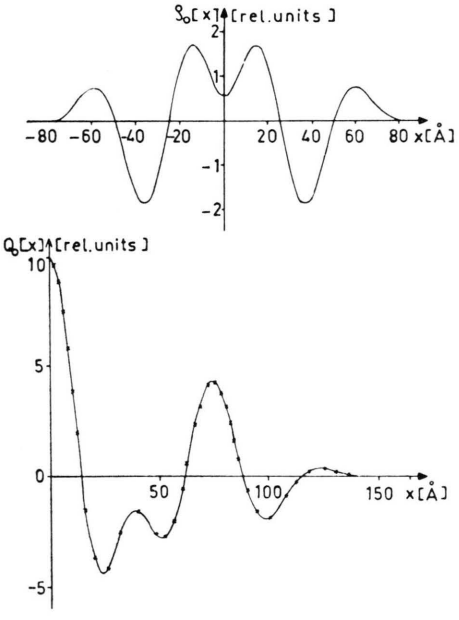

Fig. 20. Ideal electron density distribution of the double membrane and the Q_0-functions of myelin swollen in 0.8 M sucrose.

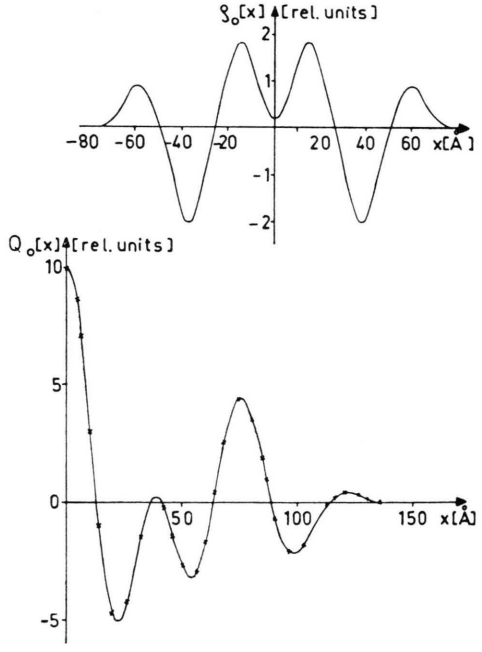

Fig. 21. Ideal electron density distribution of the double membrane and the Q_0-functions of nerve myelin swollen in 6.5% glycerol.

through comparison with the Q_0-function from a swelling experiment (or both).

The electron density profile of the double membrane in a face-to-face and back-to-back pairing obtained by deconvoluting the Q_0-functions in Fig. 22 are shown in Fig. 23. Fig. 24 shows the corresponding electron density profiles for pseudonatural myelin.

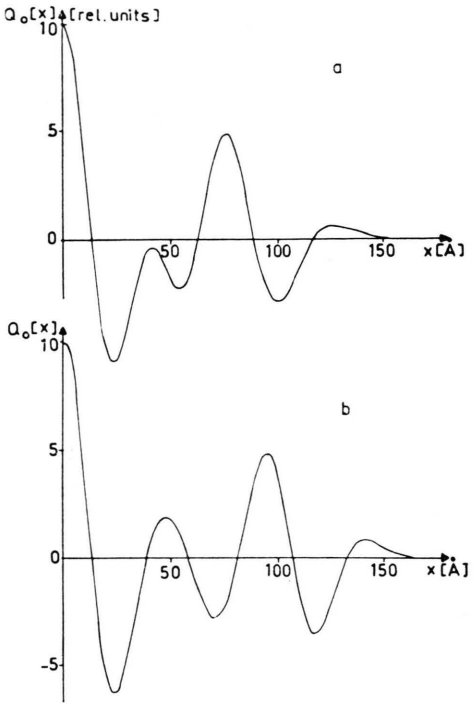

Fig. 22. The Q_0-function of the double membrane of live myelin: a) in a face-to-face coupling, b) in a back-to-back coupling.

Discussion of the Results

Various membrane parameters in the unswollen, swollen and fixed states

Our results indicate that swelling and fixation influence not only the Bragg period, but also the double membrane profile and to some extent even the single membrane profile.

The width of the membrane pair in the natural state which is about 168 – 170 Å, decreases to about 162 Å on swelling, for example, in 0.8 M sucrose. On a minute's fixation in OsO_4-vapour the double membrane width decreases considerably to about 144 to 146 Å (Table III).

There is also remarkable fluctuation in the distances between the external positive peaks of the double membrane. For live nerve, one obtains 121 Å. On a minute's fixation in OsO_4-vapour, this value decreases to 112 Å; for myelin swollen in 0.8 M sucrose the distance is approximately 118 Å, while for nerve samples swollen in 6.5% glycerol, one obtains values ranging from 110 – 120 Å.

The centre-to-centre distance between the positive peaks of the single membrane is approximately 43 Å for live nerve and 45 Å for pseudo live nerve; on one minute's fixation in OsO_4-vapour, the value decreases slightly to 41 Å, while on swelling either in 0.8 M sucrose or in 6.5% glycerol the distance increases slightly to 45 Å.

The centre-to-centre distance across the cytoplasmic interspace which is about 72 Å for live nerve increases slightly to about 75 Å for pseudo live nerve and myelin swollen in 6.5% glycerol. In 0.8 M sucrose the value is about 73 Å.

From the calculated electron density distributions, the resolution of the electron density profile, defined theoretically as $L/2n$, where L is the repeat distance and n is the number of diffraction orders used in the synthesis, was found to be approximately 22 Å for live nerve, 20 – 22 Å for fixed myelin and 16 – 22 Å for swollen nerves. The resolution is principally limited by the so-called termination effects [29].

From the comparison of various parameters for live, swollen and fixed nerves, it is evident that the assumption of an identical double membrane profile for different experimental states (natural, swollen, fixed) is not generally justifiable. Also, the assumption of a centrosymmetrical single membrane profile (Caspar and Kirschner [9]) has not been confirmed.

The phase problem for live myelin

Assuming a centrosymmetrical double membrane profile the structure amplitude $F(h)$ can only be a positive or a negative real number $\pm|F(h)|$. Thus $F(h)$ can be assigned $2^5 = 32$ possible phase combinations [2]. For live nerve, the structure amplitude of the double membrane can be defined with the centre of symmetry in either the cytoplasmic or in the extracellular interspace.

Inversion of a particular structure about the x-axis does not affect the Q_0-function. Displacement of the centre of symmetry from the cytoplasmic to extracellular interspace changes only the signs of the odd diffraction orders. However, the corresponding Q_0-functions of the electron density distributions of the image and its mirror image are not identical (see for example Fig. 22). Thus, by considering the two possible centres of symmetry, one obtains 16 different Q_0-functions as all the possible phase combinations are taken into account.

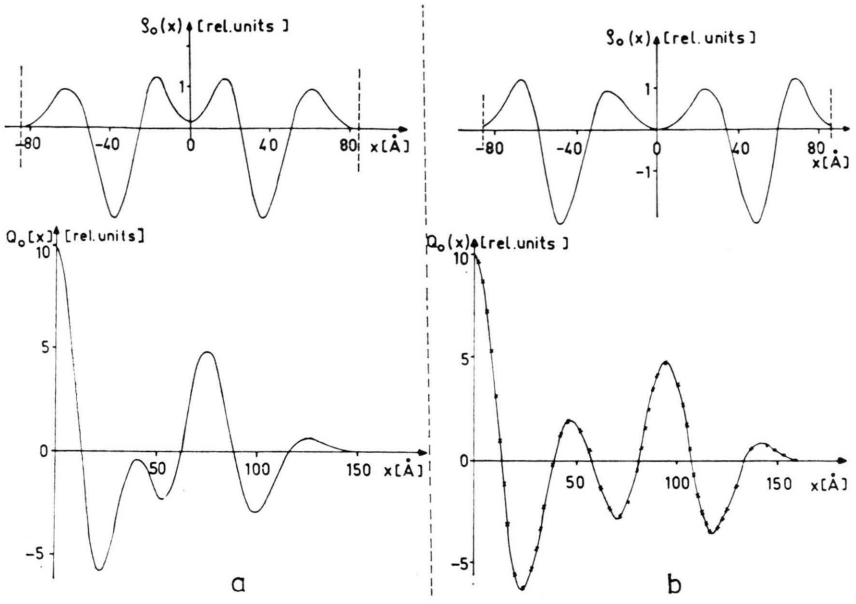

Fig. 23. The ideal electron density distribution and the Q_0-functions of the double membrane for live nerve myelin.
a) Facte-to-face (cytoplasmic pair);
b) back-to-back (extracellular pair) calculated from the Q-function of live nerve with the Phasing-In-procedure.

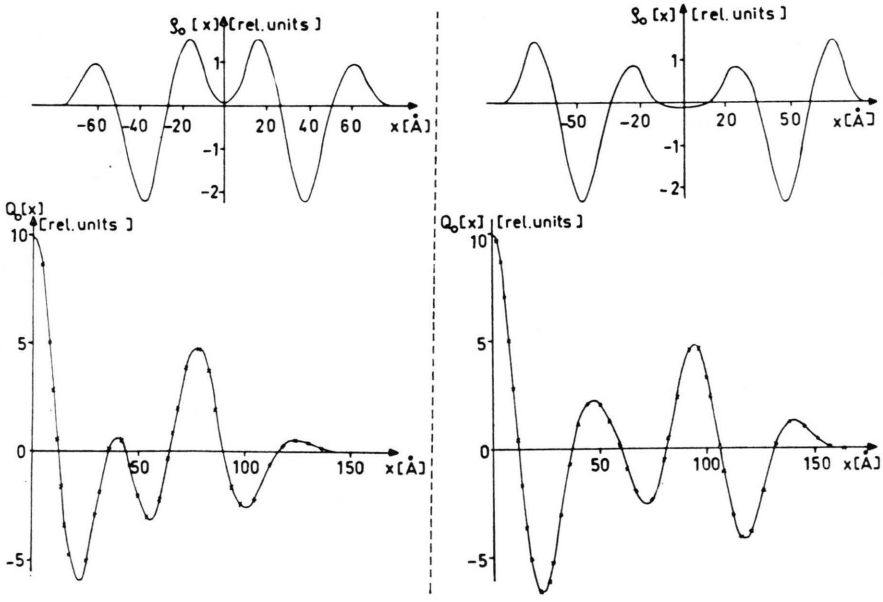

Fig. 24. The ideal electron density distribution and the Q_0-functions of the double membrane for pseudo-normal nerve myelin.
a) Face-to-face;
b) back-to-back.

By comparing all the 16 possible Q_0-functions with the Q_0-function of the double membrane obtained from a swelling experiment, one can determine immediately which Q_0-functions and thus which profiles can be eliminated. Fig. 25 shows all possible Q_0-functions with the corresponding double membrane profiles for live nerve with 5 principal reflections. Z_1 denotes the first possible centre of symmetry and Z_2 the second.

Since the electron density distribution of a membrane pair $\varrho_0(x)$ and the negative profile $-\varrho_0(x)$ have the same Q_0-function, the choice between these two structures – so-called positive and negative structures – has been made on account of relevant

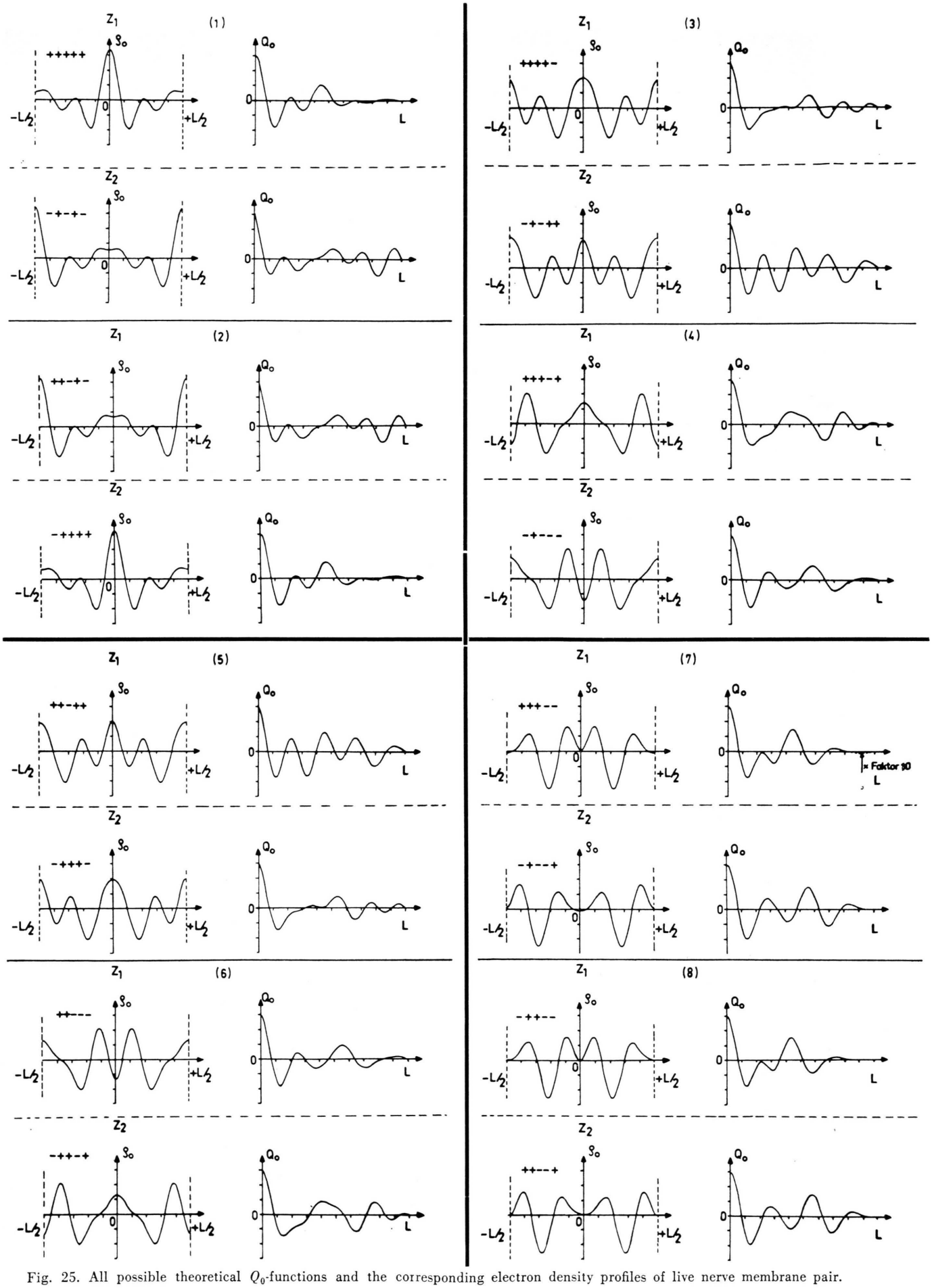

Fig. 25. All possible theoretical Q_0-functions and the corresponding electron density profiles of live nerve membrane pair.

physical factors (see for example McIntosh and Worthington [6], Gbordzoe [16]) giving a preference to the positive structure.

The application of the Fourier Analytical Deconvolution Method, taking distance statistics into account (SM-FAD-Method), permits the straight forward determination of the phase combination $-+--$ for the first five diffraction orders of live nerve for a face-to-face coupling of the double membrane (Fig. 23 a, Table V c), using only the Q-function of live nerve **.

The profile in Fig. 25 (7) is identical with the experimental condition called here pseudo-live nerve where, on account of the previous swelling, the electron density level in the extracellular interspace has been lowered slightly (Fig. 24) compared with the profile for live nerve (Fig. 23). The sign of the first diffraction order has accordingly changed from $-$ in the case of live nerve to $+$ in the case of pseudo-live nerve.

The application of the method to phase determination in the case of a higher number of diffraction orders, for example in the case of swollen nerve myelin, is obvious (Table V a, b).

It should be noted that for live nerve with 5 principal sharp reflections, there are only 8 double membrane profiles amongst the 32 possible theoretical profiles which cannot be obtained either through displacement of the centre of symmetry or through inversion of the profile about the x-axis. We refer to these 8 profiles as the fundamental electron density profiles of the double membrane of live nerve.

These 8 sets of phase combinations and their homologous solutions are shown in Table IV.

Table IV. The 8 fundamental phase sets: a) of live nerve membrane pairs and their homoloques, b), c), d).

h =	1	2	3	4	5						
		a)				b)	+	−	+	−	+
1)	−	+	−	+	−	c)	+	+	+	+	+
						d)	−	−	−	−	−
						b)	−	−	+	−	+
2)	+	+	−	+	−	c)	−	+	+	+	+
						d)	+	−	−	−	−
						b)	−	−	−	−	+
3)	+	+	+	+	−	c)	−	+	−	+	+
						d)	+	−	+	−	−
						b)	−	−	−	+	−
4)	+	+	+	−	+	c)	−	+	−	−	−
						d)	+	−	+	+	+
						b)	+	−	−	−	+
5)	−	+	+	+	−	c)	+	+	−	+	+
						d)	−	−	+	−	−
						b)	−	−	+	+	+
6)	+	+	−	−	−	c)	−	+	+	−	+
						d)	+	−	−	+	−
						b)	−	−	−	+	+
7)	+	+	+	−	−	c)	−	+	−	−	+
						d)	+	−	+	+	−
						b)	+	−	−	+	+
8)	−	+	+	−	−	c)	+	+	−	−	+
						d)	−	−	+	+	−

a) Fundamental phase combination;
b) inversion of a) about the x-axis;
c) displacement of centre of symmetry;
d) inversion of c) about the x-axis.

Phase determination and distance statistics

Table V a – e gives examples of the numerical values of the Fourier coefficients obtained by deconvoluting the Q_0-functions for normal, swollen and fixed nerves. $\delta(x-l_i)$ denotes cases where distance fluctuations between neighbouring membranes have been eliminated and $H(x-l_i)$ cases with distance fluctuations between adjacent membranes. n denotes 'diffraction order' n_{max} the highest diffraction order observed.

About 10% distance statistics in the membrane system usually results in the change of the signs of the 1st, 4th and 5th diffraction orders from *minus* in the native state to *plus* for swollen and fixed myelin. This gives rise to an electron density profile similar to those illustrated in Figs 14 a and 25, $1, Z_1$.

Concluding remarks

The method for determining the electron density of the nerve myelin described above is a direct method which not only permits correct phasing but also a qualitative and quantitative description of the effects of different swelling solutions and fixatives on the electron density distribution of the membrane. The method has a special advantage over the combined swelling and sampling method [2, 5, 10] since its application does not require several intensity functions from different experiments, nor the introduction of 'fictitious Bragg distances' [10]. The Phasing-in-Procedure is based entirely on the evaluation of a single intensity function. Phase determination is still possible even when higher dif-

** Compare with ref. [1, 2, 5, 6], where swelling, and ref [7], where fixation techniques have been employed in addition.

Tab. V. Examples of Fourier coefficients, showing the influence of distance statistics on phase determination.

a) myelin swollen in 0.8 m sucrose, $L=361$ Å, $l_i=73$ Å

k	$\delta(x-l_i)$ a_k	$H(x-l_i)$ $g_i=10\%$ a_k $(k\equiv n)$
0	0.570	0.547
1	+1.115	+1.013
2	+3.708	+3.282
3	+1.842	+2.801
4	−3.017	+2.713
5	−1.791	+1.988
6	−0.118	+0.478
7	−0.113	+0.001
8	+0.001	−0.001
9	−0.074	−0.001
$n_{max}=9$		

b) myelin swollen in 6.5% glycerol $L=299$ Å, $l_i=74.8$ Å

k	$\delta(x-l_i)$ a_k	$H(x-l_i)$ $g_i=10\%$ a_k
0	0.456	0.435
1	+1.038	+0.894
2	+3.699	+3.161
3	+0.596	+2.456
4	−3.855	+3.222
5	−1.102	+2.010
6	+0.044	+0.460
7	−0.229	−0.087
8	−0.225	−0.147
9	−0.099	−0.211
10	+0.290	−0.270
11	+0.130	−0.206
12	−	−0.086
$n_{max}=9$		

c) normal nerve $L=170$ Å, $l_i=71.8$ Å

k	$\delta(x-l_i)$ a_k
0	0.065
1	−0.185
2	+3.242
3	+2.318
4	−3.266
5	−2.208
6	+0.094
7	+0.379
8	+0.286
9	+0.001
10	−0.032
$n_{max}=5$	

d) pseudo-normal nerve $L=171$ Å, $l_i=75.8$ Å

k	$\delta(x-l_i)$ a_k $(k\equiv n)$
0	0.218
1	+0.483
2	+3.605
3	+0.668
4	−4.066
5	−1.135
6	+0.305
7	+0.162
8	−0.020
9	−0.123
10	+0.235
11	+0.112
12	−0.034
$n_{max}=5$	

e) fixed nerv: 1 min in OsO_4-vapour $L=168$ Å, $l_i=74.7$ Å

k	$\delta(x-l_i)$ a_k	$H(x-l_i)$ $g_i=10\%$ a_k
0	0.292	0.279
1	+0.784	+0.645
2	+3.454	+2.923
3	+0.035	+2.217
4	−4.131	+3.443
5	−0.432	+1.976
6	+0.388	−0.670
7	−0.464	+0.220
8	−0.167	+0.322
9	+0.118	+0.269
10	+0.405	+0.300
11	+0.073	+0.260
12	−0.082	+0.147
13	−	+0.041
$n_{max}=5$		

fraction orders in the intensity function are no longer resolved.

The uniqueness of the solution is only limited by the fact that the Q_0-function does not distinguish between the so-called positive and negative structures.

The slight line broadening in the intensity profiles of normal nerve myelin, which has hitherto been overlooked, may be attributed to several factors: Apart from instrumental factors, other factors contributing to line broadening may be the finite size of the myelin lamellae – so-called crystallite-size-broadening – and possible strain-broadening. Hitherto, the possibility of the existence of microstrains in biological membrane systems has not been investigated. Further investigations in this direction may be of interest.

The authors express their gratitude to the following: Dr. Pape for supplying the FAD programme and for very helpful discussions, Dr. Steul for introducing to us the preparation techniques, Dipl.Chem. Walter and Mrs. S. El-Deeb for valuable technical assistance.

The Scholarships Secretariat of the Government of the Republic of Ghana for financial support to Dr. M. K. Gbordzoe during the time of the above investigations.

The computer calculations where done at the computer centre (Rechenzentrum) of the University of Freiburg im Breisgau.

[1] J. B. Finean and R. E. Burge, J. Mol. Biol. **7,** 672–682 (1963).
[2] M. F. Moody, Science **142,** 1173–1174 (1963).
[3] C. R. Worthington and A. E. Blaurock, Biochim. Biophys. Acta **173,** 427–435 (1969).
[4] E. A. Blaurock, J. Mol. Biol. **56,** 35–52 (1971).
[5] C. R. Worthington and T. J. McIntosh, Nature, New Biology **245,** 97–99 (1973).
[6] T. J. McIntosh and C. R. Worthington, Biophys. J. **14,** 363–385 (1974).
[7] C. K. Akers and D. F. Parsons, Biophys. J. **10,** 101–136 (1970). – Reply to "Myelin membrane structure by X-ray diffraction" by David Harker, Biophys. J. **12,** 1296–1301 (1972).
[8] D. Harker, Biophys. J. **12,** 1285–1294 (1972).
[9] D. L. D. Caspar and D. A. Kirschner, Nature, New Biology **231,** 46–52 (1971).
[10] C. R. Worthington and T. J. McIntosh, Biophys. J. **14,** 703–730 (1974).
[11] R. Hosemann and S. N. Bagchi, Direct Analysis of Diffraction by Matter, North Holland Publishing Co. 1962.
[12] A. Hybl, J. Appl. Cryst. **10,** 141–146 (1977).
[13] A. E. Blaurock and J. C. Nelander, J. Mol. Biol. **103,** 421 (1976).
[14] D. W. Marquart, J. Soc. Indust. Math. **11,** 431 (1963).
[15] E. H. Pape, Biophys. J. **14,** 284–294 (1974).
[16] M. K. Gbordzoe, Dissertation, Univerity of Freiburg im Breisgau 1977.
[17a] W. Kreutz, Habilitationschrift, Technische Universität Berlin 1968.
[17b] W. Kreutz, Advances in Botanical Research, **vol. 3** (R. D. Preston, ed.), Academic Press, New York 1970.
[18] W. Lesslauer, J. E. Cain, and J. K. Blasie, Biochim. Biophys. Acta **241,** 547 (1971).
[19] H. Margenau and G. M. Murphy, The Mathematics of Physics and Chemistry, p. 261–262, D. van Nostrand Co., Princeton, New Jersey 1956.
[20] W. Kreutz and E. H. Pape, Evaluation of X-Ray Diffraction Patterns of Biomembrane Systems. Summer Institute on the Physics of Biological Membranes, Alta Lake, Canada, British Columbia 1974.
[21] B. K. Vainshtein, Diffraction of X-Ray by Chain Molecules, Elsevier Publishing Co., Amsterdam 1966.
[22] M. J. Buerger, Vector Space. Its Application in Crystal Structure Investigation, p. 18–19, John Wiley and Sons Inc., New York 1959.
[23] H. Lipson and W. Cochran, Determination of Crystal Structure in the Crystalline State, **Vol. III,** pp. 11–12, Bell and Sons, London 1968.
[24] L. V. Azároff, Elements of X-Ray Crystallography, Mc Graw-Hill Book Co., New York 1968.
[25] H. Kiessig, Kolloid Z. **98,** 213 (1942).
[26] O. Kratky, Z. Elektrochemie **58,** 49–53 (1954).
[27] R. Bonart and R. Hosemann, Kolloid W., Z. Polymere **186,** 16 (1962).
[28] R. Hosemann, J. Appl. Phys. **34,** 25 (1963).
[29] H. Neff, Grundlagen und Anwendungen der Röntgenstrukturanalyse, Oldenbourg Verlag, München 1962.
[30] E. H. Pape, K. Klott, and W. Kreutz, Biophys. J. **19,** 141 (1977).
[31] S. Schwartz, J. E. Cain, E. A. Dratz, and J. K. Blasie, Biophys. J. **15,** 1201 (1975).
[32] G. H. Stout and L. H. Jensen, X-Ray Structure Determination, p. 326, The McMillan Co., New York 1968.